TITLE:

From path integrals to tensor networks for the AdS/CFT correspondence

AUTHOR(S):

Miyaji, Masamichi; Takayanagi, Tadashi; Watanabe, Kento

From path integrals to tensor networks for the AdS/CFT correspondence

Masamichi Miyaji,[1] Tadashi Takayanagi,[1,2] and Kento Watanabe[1]

[1]*Center for Gravitational Physics, Yukawa Institute for Theoretical Physics (YITP), Kyoto University,
Kyoto 606-8502, Japan*
[2]*Kavli Institute for the Physics and Mathematics of the Universe (Kavli IPMU), University of Tokyo,
Kashiwa, Chiba 277-8582, Japan*

In this paper, we discuss tensor network descriptions of AdS/CFT from two different viewpoints. First, we start with a Euclidean path-integral computation of ground state wave functions with a UV cutoff. We consider its efficient optimization by making its UV cutoff position dependent and define a quantum state at each length scale. We conjecture that this path integral corresponds to a time slice of anti–de Sitter (AdS) spacetime. Next, we derive a flow of quantum states by rewriting the action of Killing vectors of AdS_3 in terms of the dual two-dimensional conformal field theory (CFT). Both approaches support a correspondence between the hyperbolic time slice H_2 in AdS_3 and a version of continuous multiscale entanglement renormalization ansatz. We also give a heuristic argument about why we can expect a sub-AdS scale bulk locality for holographic CFTs.

I. INTRODUCTION

Even though the holographic principle [1], especially the AdS/CFT correspondence [2], is expected to provide us with an extremely powerful method to understand quantum gravity, its basic mechanism has remained mysterious. One interesting possibility of explaining the mechanism of holography is its possible connections to tensor networks. Tensor networks are methods to express quantum wave functions in terms of network diagrams and are in a very similar spirit to holography because they geometrize algebraically complicated quantum states.

In the pioneering work [3], it has been conjectured that the AdS/CFT correspondence may be interpreted as the multi-scale entanglement renormalization ansatz (MERA) network [4,5], which is a particular example of tensor networks for conformal field theories (CFTs). At an intuitive level, this fits nicely with the AdS/CFT in that the MERA network is aimed at an explicit real space renormalization group (RG) flow in terms of RG evolution of quantum states. Moreover, estimations of entanglement entropy of MERA networks done in [4] look analogous to the holographic entanglement entropy [6], realizing emergent spacetimes from quantum entanglement (for recent reviews see [7,8]). Such a connection to tensor networks can also be strongly suggested by the recent reformulation of holographic entanglement entropy in terms of bit threads [9].

The tensor network is defined in a discretized lattice such as spin systems and to connect the actual AdS/CFT we need to take a continuum limit. A candidate of a continuum version of MERA is formulated in [10] and is called continuous MERA (cMERA). It was conjectured in [11,12] that the AdS/CFT can be regarded as a cMERA network. Even though the special conformal invariance is

not realized in the MERA network, cMERA has an advantage that this symmetry is clearly realized.

In the original argument [3], the MERA network was considered to describe the canonical time slice of AdS_{d+2}, i.e. hyperbolic space H_{d+1}. However later, it has been pointed out by several authors [13–16] that the MERA network may correspond to a de Sitter spacetime dS_{d+1} instead of hyperbolic space, especially from the viewpoint of its causal structure of MERA. Note that a hyperbolic space and de Sitter spacetime have the same isometry $SO(1, d+1)$ and it is not easy to distinguish them only by symmetries. In the paper [14], the MERA tensor network is argued to describe a space called kinematical space, which is nonlocally related to the original AdS spacetime with mathematically rich structures [17].

Nevertheless, we are still attempting to interpret an AdS spacetime itself as a continuous limit of a certain tensor network [a continuous tensor network (cTN)]. A quantum state is time evolved by a given Hamiltonian and this is also described by a network of unitary transformations. Thus we can have a tensor network description of whole spacetime if each time slice, which defines a quantum state, is described by a tensor network. A powerful advantage of tensor network description is that we can take a subregion inside the network and define a quantum state by contracting tensors. Motivated by this, in [18], it was conjectured that in any spacetime described by Einstein gravity, each codimension two convex surface corresponds to a quantum state in the dual theory, called surface/state correspondence. This largely extends the holographic principle as it can be applied to gravitational spacetime without any boundaries. The perfect tensor network [19] (see also a closely related network using random tensors [20]), found from a relation between quantum error correcting codes and holography,

provides an explicit toy example for the surface/state correspondence. Moreover, it is expected to provide a tensor network which corresponds to the hyperbolic space H_2 rather than the de Sitter spacetime. Indeed, it has a discretized version of the full conformal symmetry. Even though this network respects the isometry of AdS_3 and holographic entanglement entropy, the quantum state itself has a flat entanglement spectrum and thus deviates from any vacuum of CFTs.

To understand connections between tensor networks and AdS/CFT better, in this paper we study the AdS_3/CFT_2 duality from two different viewpoints: (i) Euclidean path-integral description of wave function with a position dependent cutoff, and (ii) $SL(2, R)$ transformations of AdS_3 in surface/state correspondence. We see that both approaches support the correspondence between a hyperbolic time slice in AdS_3 and a cMERA-like network for a CFT vacuum. The second approach also shows that we can equally identify the network with a de Sitter slice. Next we turn to the excited states. Especially we focus on the locally excited state in the bulk AdS_3 and cTN description of its CFT dual. As we see below, we find a consistent picture which reveals a structure similar to the perfect tensor network [19] and the random tensor network [20]. Finally we give a heuristic argument about why we expect a sub-AdS scale bulk locality for holographic CFTs. In this paper we mainly consider two-dimensional CFTs for simpler presentations. However, many results can be generalized into the higher dimensional AdS/CFT.

This paper is organized as follows. In Sec. II, we give a brief review of AdS_3 geometry and its global symmetry. In Sec. III, we study a Euclidean path-integral description of vacuum wave function of two-dimensional CFT and introduce a position dependent cutoff, which preserves the conformal symmetries. We argue that this corresponds to the time slice of AdS space. Following this approach we calculate a wave function at each length scale. In Sec. IV, we review the formulation of cMERA with several updates. In Sec. V, we identify a continuous tensor network which describes the global AdS_3 spacetime via the Killing symmetry of the AdS space. In Sec. VI, we give a heuristic argument about why we expect a sub-AdS scale bulk locality for holographic CFTs. In Sec. VII, we examine locally excited states in the bulk in our continuous tensor network description. In Sec. VIII, we summarize our conclusions and discuss future problems. In Appendix A, we present details of several choices of cutoff functions in Euclidean path integrals. In Appendix B, we extend the construction of cMERA to present a formulation of continuous tensor networks which describe a holographic spacetime and show consistency conditions.

When we were completing this paper, we noticed a very interesting paper [21] where a connection between continuous tensor networks and wave functions in the Euclidean path integral with a UV cutoff have been studied.

The path-integral formulation in our paper is different from theirs in that we made the UV cutoff position dependent. Appendix A in this paper includes a consistency between our work and [21].

II. ADS₃ GEOMETRY

In this section, we briefly review basic properties of the AdS_3 geometry, which are important in our later arguments. The Lorentzian AdS_3 space with a radius L is defined by the hypersurface in $R^{2,2}$,

$$X_0^2 + X_3^2 = X_1^2 + X_2^2 + L^2. \tag{1}$$

The global AdS_3 (with radius L) is defined by the parametrization

$$\begin{aligned}
X_0 &= L \cosh\rho \cos t, \\
X_3 &= L \cosh\rho \sin t, \\
X_1 &= L \sinh\rho \sin\phi, \\
X_2 &= L \sinh\rho \cos\phi. \tag{2}
\end{aligned}$$

This leads to the following metric:

$$ds^2 = L^2(-\cosh^2\!\rho\, dt^2 + d\rho^2 + \sinh^2\!\rho\, d\phi^2). \tag{3}$$

The Euclidean global AdS_3 (i.e. H_3) is obtained by the Wick rotation $t \to it$.

Sometimes it is also useful to work with the Poincare AdS metric

$$ds^2 = L^2 \frac{dz^2 - d\tau^2 + dx^2}{z^2}, \tag{4}$$

in our later arguments.

A. Global symmetry

The AdS_3 space (3) has the $SL(2, R)_L \times SL(2, R)_R$ symmetry, which is generated by (L_1, L_0, L_{-1}) and $(\tilde{L}_1, \tilde{L}_0, \tilde{L}_{-1})$. They correspond to the (global) Virasoro symmetry of its dual two-dimensional CFT. These are explicitly given by the following Killing vectors in AdS_3 [22],

$$L_0 = i\partial_+, \qquad \tilde{L}_0 = i\partial_-,$$

$$L_{\pm 1} = ie^{\pm ix^+}\left[\frac{\cosh 2\rho}{\sinh 2\rho}\partial_+ - \frac{1}{\sinh 2\rho}\partial_- \mp \frac{i}{2}\partial_\rho\right],$$

$$\tilde{L}_{\pm 1} = ie^{\pm ix^-}\left[\frac{\cosh 2\rho}{\sinh 2\rho}\partial_- - \frac{1}{\sinh 2\rho}\partial_+ \mp \frac{i}{2}\partial_\rho\right], \tag{5}$$

where $x^\pm \equiv t \pm \phi$ and $\partial_\pm \equiv \frac{\partial}{\partial x^\pm}$.

Notice that a $SL(2,R)$ subgroup of $SL(2,R)_L \times SL(2,R)_R$ preserves the time slice $t = 0$. It is generated by $l_n \equiv L_n - \tilde{L}_{-n}(n = 0, -1, 1)$, i.e.

$$l_0 = L_0 - \tilde{L}_0 = i\partial_\phi,$$

$$l_{-1} = L_{-1} - \tilde{L}_1 = ie^{-i\phi}\left[\frac{1 + \cosh(2\rho)}{\sinh(2\rho)}\partial_\phi + i\partial_\rho\right],$$

$$l_1 = L_1 - \tilde{L}_{-1} = -ie^{i\phi}\left[-\frac{1 + \cosh(2\rho)}{\sinh(2\rho)}\partial_\phi + i\partial_\rho\right]. \quad (6)$$

Indeed they satisfy the $SL(2,R)$ algebra and correspond to Killing vectors of the hyperbolic space H_2,

$$ds^2 = L^2(d\rho^2 + \sinh^2\rho d\phi^2). \quad (7)$$

We can identify the geometrical action with a linear combination of l_n as follows:

$$i\partial_\rho = -\frac{i}{2}(e^{i\phi}l_{-1} - e^{-i\phi}l_1),$$

$$i\partial_\phi = l_0. \quad (8)$$

The $SL(2,R)$ transformation $g(\rho,\phi)$ which takes the origin $\rho = 0$ to a point (ρ,ϕ) on H_2 is given by

$$g(\rho,\phi) = e^{-i\phi l_0}e^{\frac{\rho}{2}(l_1 - l_{-1})}. \quad (9)$$

B. Hyperbolic/de Sitter slices in AdS$_3$

If we parametrize the hypersurface (1) as follows,

$$X_0 = L\sinh\tau\sinh\eta,$$
$$X_3 = L\cosh\eta,$$
$$X_1 = L\cosh\tau\sinh\eta\sin\phi,$$
$$X_2 = L\cosh\tau\sinh\eta\cos\phi, \quad (10)$$

then we find the metric

$$ds^2 = L^2(d\eta^2 + \sinh^2\eta(-d\tau^2 + \cosh^2\tau d\phi^2)). \quad (11)$$

This shows that a constant η slice is a two-dimensional de Sitter spacetime, which is accommodated in the interval $-\pi < t < 0$. If we take the $\eta = 0$ limit, it becomes a light cone. To go beyond this, we can introduce the following coordinate,

$$X_0 = L\cosh\tau\sin\eta,$$
$$X_3 = L\cos\eta,$$
$$X_1 = L\sinh\tau\sin\eta\sin\phi,$$
$$X_2 = L\sinh\tau\sin\eta\cos\phi, \quad (12)$$

which leads to

$$ds^2 = L^2(-d\eta^2 + \sin^2\eta(d\tau^2 + \cosh^2\tau d\phi^2)). \quad (13)$$

This describes the hyperbolic slices of AdS$_3$.

If we consider the Euclidean AdS$_3$ ($= H_3$) defined by

$$X_0^2 = X_1^2 + X_2^2 + X_3^2 + L^2, \quad (14)$$

we can set

$$X_0 = L\cosh\tau\cosh\eta,$$
$$X_3 = L\sinh\eta,$$
$$X_1 = L\sinh\tau\cosh\eta\sin\phi,$$
$$X_2 = L\sinh\tau\cosh\eta\cos\phi, \quad (15)$$

to reach the metric

$$ds^2 = L^2(d\eta^2 + \cosh^2\eta(d\tau^2 + \sinh^2\tau d\phi^2)). \quad (16)$$

This describes a hyperbolic slice of Euclidean AdS$_3$.

III. ADS/CFT FROM THE EUCLIDEAN PATH INTEGRAL

In this section, we study the Euclidean path-integral description of ground state wave functions of two-dimensional CFTs. We introduce UV cutoff efficiently in a conformal invariant way and show that we can deform the path integral into that on a hyperbolic space H$_2$. We argue that this hyperbolic space corresponds to a time slice of AdS$_3$.

A. Euclidean path integral with UV cutoff

Consider a two-dimensional CFT on R^2. We define the coordinate of R^2 to be (z, x), where z is the Euclidean time. We simply express all fields in the CFT as $\phi(z,x)$. The ground state wave function $\Psi[\phi(x)]$, which is not normalized, is written as a Euclidean path integral,

$$\Psi[\phi(x)] = \int\prod_{z_0 < z < \infty}D\phi(z,x)\cdot\delta(\phi(z_0,x)$$
$$= \phi(x))\cdot e^{-S_{\text{CFT}}(\phi)}. \quad (17)$$

To make an explicit analysis, let us consider a free scalar field theory as a toy example,

$$S_{\text{CFT}} = \int dxdz\mathcal{L}_{\text{CFT}} = \int dxdz[(\partial_z\phi)^2 + (\partial_x\phi)^2]. \quad (18)$$

With the boundary condition $\phi(0,x) = \phi(x)$ we can solve the equation of motion $(\partial_x^2 + \partial_z^2)\phi = 0$ as follows:

$$\phi(z,x) = \int_{-\infty}^{\infty} dk \phi(k) e^{ikx-|k|z}, \qquad (19)$$

where $\phi(k)$ is the Fourier transformation of $\phi(x)$. Note that here we assumed that there is no singular behavior in the limit $z \to \infty$.

The on-shell action is evaluated as

$$S_{\text{on shell}} = 4\pi \int_0^{\infty} dz \int_{-\infty}^{\infty} dk |k|^2 e^{-2|k|z} \phi(k) \phi(-k)$$
$$= 2\pi \int_{-\infty}^{\infty} dk |k| \phi(k) \phi(-k). \qquad (20)$$

Since the path integral of quantum fluctuation only gives an overall constant factor (see e.g. [23]), the wave function is evaluated as

$$\Psi[\phi(x)] \propto e^{-S_{\text{on shell}}} = e^{-2\pi \int_{-\infty}^{\infty} dk |k| \phi(k) \phi(-k)}, \qquad (21)$$

reproducing the well-known result.

In this analysis we observe an important fact that in the k integral at fixed z in (20), only modes with $|k| \lesssim 1/z$ contribute. This fact allows us to approximate the path integral by introducing a z dependent cutoff of the momentum without changing the final result of the wave function as depicted in Fig. 1. This is realized by putting a cutoff function $\Gamma(\lambda|k|z)$ in the path integral. λ is a parameter which controls our approximation. We simply define it such that $\Gamma(x) = 1$ if $|x| < 1$; otherwise $\Gamma(x) = 0$, though in our argument, the precise form of the cutoff function $\Gamma(x)$ does not play an important role. The resulting wave function $\Psi[\phi(x)]$ remains approximately the same even if we introduce this z dependent cutoff as we confirm below.

Let us introduce a length scale (z_0) dependent wave function $\Psi_{z_0}[\phi(x)]$ by the Euclidean path integral for the range $z_0 \leq z < \infty$ in the presence of the cutoff $\Gamma(\lambda|k|z)$. Since $\phi(x)$ is defined by the value $\phi(z_0, x)$, we need to rescale the scalar field as $\phi \to e^{|k|z_0}\phi$ as is clear from (19). Finally we obtain
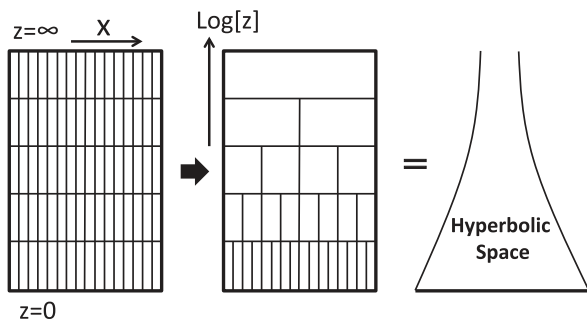

FIG. 1. A computation of ground state wave function from the Euclidean path integral and its optimization, which is described by a hyperbolic geometry.

$$\Psi_{z_0}[\phi(x)] \propto e^{-2\pi \int_{-\frac{1}{\lambda z_0}}^{\frac{1}{\lambda z_0}} dk |k| (1-e^{2|k|z_0-2/\lambda}) \phi(k) \phi(-k)}. \qquad (22)$$

First of all, it is obvious that the function (22) at $z_0 = 0$ coincides with the correct vacuum wave function (21) assuming $\lambda \ll 1$. In principle, we can also multiply the factor $(1 - e^{-2/\lambda})^{-1}$ on the cutoff function so that we get the correct wave function at $z_0 = 0$ even when λ is $O(1)$. Having this in mind we simply set $\lambda = 1$ below.

Alternatively, we can improve this procedure by taking into account contributions from high momentum modes in a nonlocal way. Let us, for example, replace the cutoff function as follows:

$$\Gamma(|k|z) \to f(|k|z) \equiv \Gamma(|k|z) + \frac{1}{2}(1 - \Gamma(|k|z)) \cdot e^{|k|z-1}, \qquad (23)$$

where we chose this such that the higher momentum modes $|k|z_0 \gg 1$ are suppressed in the path integral.

As we analyze in detail in Appendix A [as the example (ii)], in this case, the high momentum contribution cancels the extra term $\sim e^{2|k|z_0-2/\lambda}$ in (22) when $|k|z_0 < 1$. Finally the wave function at length scale z_0 reads

$$\Psi_{z_0}[\phi(x)] \propto e^{-2\pi \int_{|k| \leq 1/z_0} dk |k| \phi(k) \phi(-k)}$$
$$\times e^{-2\pi \int_{|k| > 1/z_0} dk |k| e^{|k|z_0-1} \phi(k) \phi(-k)}. \qquad (24)$$

Note that for the modes below the cutoff, this reproduces the correct vacuum wave function (21). On the other hand, it is clear that the higher momentum modes $|k|z_0 \gg 1$ are exponentially suppressed. Thus this wave function (24) possesses the desired property.

In summary, for a finite value of z_0, wave function (22) or (24) describes the ground state below the cutoff. On the other hand, for much higher momentum modes, it becomes trivial and thus it describes a state without any real space entanglement (i.e. boundary state, as we explain in the next section).[1] This nicely describes the effective wave function at the length scale z_0 under a real space renormalization group flow.[2]

If we imagine various ways to discretize our Euclidean path integral, this z dependent UV cutoff provides us with an efficient choice for this procedure. We call this

---

[1]The wave function (22) corresponds to the boundary state with Neumann boundary condition, while the wave function (24) describes the Dirichlet one. For more details, refer to Appendix A.

[2]As we argue in Sec. III B, in a two-dimensional holographic CFT with a large central charge c, the actual momentum cutoff at the length scale z_0 is estimated to be $|k| \lesssim \frac{c}{z_0}$ (instead of $|k| \lesssim \frac{1}{z_0}$). Therefore the momentum region $\frac{1}{z_0} \lesssim |k| \lesssim \frac{c}{z_0}$ is physically meaningful and is described by a nonlocal field theory.

an optimized Euclidean path integral below. If we consider K sites in the UV theory (corresponding to $z = \epsilon$), we have $\sim K \cdot (\epsilon/z)$ sites as z grows. Therefore we can associate the following metric of H_2,

$$ds^2 = \frac{dz^2 + dx^2}{z^2}, \tag{25}$$

to the Euclidean path integral with the UV cutoff. This metric is defined such that the area measured by the metric gives the number of discretized sites. The metric (25) in the x direction is obvious from the cutoff function $\Gamma(|k|z)$. The metric in the z direction can be fixed by requiring that the vacuum state is invariant under the $SL(2, R)$ conformal symmetry generated by $l_0, l_{\pm 1}$. Note that this symmetry action preserves the boundary $z = 0$, where we define the wave function. In other words, the discretized lattice which corresponds to our Euclidean path integral is invariant under this $SL(2, R)$ transformation.

The cutoff function can also be made manifestly conformally invariant by replacing $\Gamma(|k|z)$ with $\Gamma(z \cdot k_{H_2})$, where $k_{H_2} = \sqrt{k_x^2 + k_z^2}$ is the magnitude of the wave vector of the field configuration at each point of (z, x). This cutoff $\Gamma(z \cdot k_{H_2})$ is interpreted as the discretization of (z, x) space such that each cell has the same infinitesimal area following the hyperbolic metric (25). For example, we can take an action for our optimized Euclidean path integral to be schematically as follows:

$$S_{\text{opt}} = \int dx dz \Gamma(z \cdot k_{H_2}) \mathcal{L}_{\text{CFT}}, \tag{26}$$

where the cutoff function $\Gamma(z \cdot k_{H_2})$ is acted on all fields in the CFT. In the next subsection, we argue that the hyperbolic space (25) corresponds to a time slice of Euclidean AdS$_3$ as a consequence of AdS/CFT.

Next we compactify the spacial coordinate x and express it as ϕ with the periodicity $\phi \sim \phi + 2\pi$. The ground state wave function is described by the Euclidean path integral on the upper half of the infinite cylinder $0 < z < \infty$. We can introduce a z dependent UV cutoff as before without chaining the final wave function. This leads to a discretized path integral on the Poincare disk with the metric

$$ds^2 = \frac{4 d\zeta d\bar{\zeta}}{(1 - |\zeta|^2)^2}, \tag{27}$$

where

$$\zeta = e^{-z + i\phi}. \tag{28}$$

This metric is invariant under $SL(2, R)$ transformation $l_n = L_n - \tilde{L}_{-n} (n = 0, \pm 1)$ with

$$L_n = -\zeta^{n+1} \frac{\partial}{\partial \zeta}, \qquad \tilde{L}_n = -\bar{\zeta}^{n+1} \frac{\partial}{\partial \bar{\zeta}}. \tag{29}$$

Again we observe that the metric (27) agrees (up to an overall factor) with that of the time slice of Euclidean global AdS$_3$ [refer to (3)] with the identification $\sinh \rho = \frac{2|\zeta|}{1 - |\zeta|^2}$. Moreover, the $SL(2, R)$ generators $l_0, l_{\pm 1}$ coincide with (6).

B. Interpretations in terms of AdS/CFT

As we already noted, the geometries of optimized Euclidean path integrals reproduce the time slice of Euclidean AdS spacetime as in (25) and (27). More precisely their metrics differ by a factor L^2, which is $\sim c^2$ in the Planck scale unit, from the actual AdS metric. A heuristic explanation is as follows (see also Sec. VI). Holographic CFTs are characterized by the large central charge c and a large spectrum gap [24]. Here we turn to a simple tractable model which captures these properties: a symmetric product CFT with a large central charge c on a cylinder. In such a model, the long string sector, which dominates the microstate degeneracy, can be effectively described by a CFT with a $O(1)$ central charge on a cylinder with the extended radius $O(c)$ [25]. Thus this gives a very fine-grained momentum quantization $P \sim n/c (n \in Z)$ instead of $P \sim n$. In the real space, this means that the lattice spacing is smaller by a factor $\sim c$. Therefore, the actual numbers of lattice sites per unit area in the metric (25) and (27) are $\sim c^2$. This reproduce the correct AdS$_3$ metric up to $O(1)$ constant.

In the Euclidean AdS$_3$, we can actually find infinitely many other hyperbolic slices parametrized by η in (16). Since each of them has a different radius (given by $L \cosh \eta$), it is natural to interpret that they correspond to different choices of the cutoff function,

$$\Gamma\left(\frac{z \cdot k_{H_2}}{\cosh \eta} \right). \tag{30}$$

In the coordinate system (16), we can regard η as an extra dimension and the AdS boundary as $\eta = \pm\infty$. In this interpretation, following a standard understanding of AdS/CFT (refer to [26,27] for studies of gravity dual of CFTs on AdS spaces), the evolution of η can be regarded as a RG flow such that the momentum scale is given by $\cosh \eta$. This consideration also justifies the action (26) at $\eta = 0$.

Let us study the field theory more carefully by using the improved UV cutoff $f(|k|z)$ given by (23). Our argument in the above shows that in a two-dimensional holographic CFT with a large central charge c, the actual momentum cutoff at the length scale z is estimated to be $|k| \lesssim \frac{c}{z}$, instead of $|k| \lesssim \frac{1}{z}$. Therefore for the momentum region $\frac{1}{z} \lesssim |k| \lesssim \frac{c}{z}$, we expect a very nonlocal theory whose action for the free scalar is given by $S = \int dx dz \phi \cdot f(|k_{H_2}|z) \cdot \phi$, or more

generally by (26) with $\Gamma(|k|z)$ replaced with $f(|k|z)$. On the other hand, we can physically ignore the existence of modes above this strict UV cutoff $|k| \gtrsim \frac{c}{z}$.

This nonlocality occurs when we consider a small structure such that $z \gtrsim \Delta x$. For example, consider the entanglement entropy S_A at a fixed (Euclidean time) z with respect to a subsystem A given by an interval with the length Δx. If $\Delta x \ll z$, then we expect the volume law due to the nonlocality (see [28,29] for an explicit example in such a nonlocal scalar field theory),

$$S_A \sim c \frac{\Delta x}{z}, \qquad (31)$$

where we used the fact that the effective lattice spacing is estimated as z/c. This agrees with the holographic computation in the Poincare AdS$_3$ as the minimal surface almost coincides with the original interval A if $\Delta x \ll z$. This is an additional support for our argument. Refer also to Fig. 2 for another explanation of (31) by using a MERA tensor network.

Finally we emphasize again that the above argument can be applied only to large c CFTs. For example, if we consider a CFT with a central charge $O(1)$, the strict UV cutoff is given by $|k| \leq 1/z$ and thus we cannot reach the volume law phase (31).
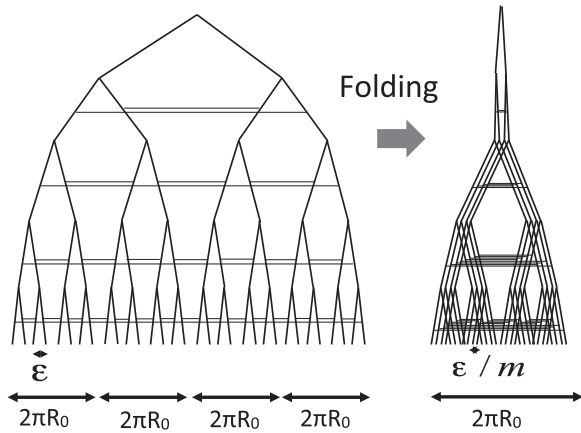

FIG. 2. Folding the MERA network in a two-dimensional symmetric product CFT M^m/S_m (we chose $m = 4$.). The left picture expresses a MERA network for a long string sector vacuum which is equivalent to the single string sector vacuum with the radius $mR_0 = 4R_0$. The right picture describes its equivalent network after the folding such that the radius is R_0. We show the coarse graining (isometries) as trivertices and the disentanglers (unitary transformations) as horizontal lines. The right network shows that the actual lattice spacing is ϵ/m. From this network, we can easily see that the entanglement entropy S_A follows the volume law for a small interval A with the width $(\epsilon/m \ll)\Delta x \ll \epsilon$ in the large c limit $m \to \infty$. Note also that the final MERA network is squeezed near the top region (roughly more than $\log \frac{R_0}{\epsilon}$ steps from the bottom). This is very analogous to the global AdS$_3$ metric.

C. Einstein-Rosen bridge from the path integral

Another interesting example is the quantum state in the thermofield double CFT given by

$$|\Psi_{TFD}\rangle \propto \sum_n e^{-\frac{\beta}{4}(H_1 + H_2)}|n\rangle_1 |n\rangle_2. \qquad (32)$$

In the Euclidean path-integral formalism, the wave function for this state is described by a path integral on a cylinder with a finite width, $-\frac{\beta}{4} < z < \frac{\beta}{4}$, in the Euclidean time direction (we set the UV cutoff z_0 to 0 for simplicity). We express the spacial coordinate as x.

Again we consider a free scalar field theory as a toy model for our explanation. We introduce the boundary conditions for the two boundaries at $z = \pm\frac{\beta}{4}$ for the field $\phi(z, x)$,

$$\phi\left(-\frac{\beta}{4}, x\right) = \phi_1(x), \qquad \phi\left(\frac{\beta}{4}, x\right) = \phi_2(x). \qquad (33)$$

The classical solution to the equation of motion $(\partial_x^2 + \partial_z^2)\phi = 0$ is given by

$$\phi(x, z) = \int_{-\infty}^{\infty} dk \left[\phi_+(k)e^{ikx} \frac{\cosh(|k|z)}{\cosh(|k|\beta/4)} - \phi_-(k)e^{ikx} \frac{\sinh(|k|z)}{\sinh(|k|\beta/4)} \right], \qquad (34)$$

where $\phi_\pm(k)$ is the Fourier transformation of $\frac{1}{2}(\phi_1(x) \pm \phi_2(x))$.

From this expression, we can estimate the effective momentum cutoff as

$$|k| \lesssim \max\left\{ \frac{1}{|z + \beta/4|}, \frac{1}{|z - \beta/4|} \right\}. \qquad (35)$$

Therefore it is clear that near the two boundaries $z = \pm\frac{\beta}{4}$, the metric of the discretized path integral behaves like $ds^2 \propto \frac{dz^2 + dx^2}{(z \pm \beta/4)^2}$. The space gets maximally squeezed at the middle $z = 0$. To find the precise metric, we require the $SL(2, R)$ conformal symmetry, which leads to the metric

$$ds^2 = d\rho^2 + \cosh^2 \rho d\phi^2, \qquad (36)$$

with the coordinate transformation

$$\tan\left(\frac{\pi z}{\beta}\right) = \tanh\left(\frac{\rho}{2}\right). \qquad (37)$$

The SL(2,R) symmetry is explicitly given by

$$l_0 = \partial_\phi,$$
$$l_{-1} = e^\phi \left(\frac{\cosh 2\rho - 1}{\sinh 2\rho} \partial_\phi - \partial_\rho \right),$$
$$l_1 = e^{-\phi} \left(\frac{\cosh 2\rho - 1}{\sinh 2\rho} \partial_\phi + \partial_\rho \right). \qquad (38)$$

The metric (36) coincides with the time slice of the BTZ black hole i.e. the Einstein-Rosen bridge, which is known to be dual to the thermofield double state (32) [30].

D. More general backgrounds

Now we turn to a Euclidean path-integral description of more general states. First, let us introduce a mass gap. For example, consider adding the mass term $m^2 \phi^2$ in (18). Then the factor $e^{-|k|z}$ in (19) is replaced with $e^{-\sqrt{k^2+m^2}z}$. This shows that we can ignore the path integral for the region $z \gg 1/m$. Thus for an optimized lattice computation, the region $z \gg 1/m$ should be removed. This is qualitatively consistent with time slices of holographic geometries dual to confining gauge theories.

Next consider a static excited state in a CFT such as the primary state. We can insert a primary field at $z = \infty$ and perform the path integral until we reach $z = 0$. As in previous sections, we can introduce the z dependent UV cutoff without changing the final wave function, which makes discretized computations efficient. Since in such an example, the $SL(2, R)$ conformal symmetry is broken and thus quantitative analysis is not straightforward, we briefly discuss only qualitative aspects here. In general, to describe excited states we need more discretized lattices and the associated metric is increased compared with that for the vacuum. This is because to describe an insertion of operator at $z = z_1$ with a high momentum scale such that $k_1 z_1 \gg 1$, the original UV cutoff $\Gamma(|k|z)$ is not enough and should be fine grained. To describe deconfined states ($\Delta > \frac{c}{24}$), we need large number $\sim 2\pi\sqrt{c\Delta/6}$ of lattice sites even at $z = \infty$. Therefore in this case $z = \infty$ is interpreted as a black hole horizon.

More generally, if we consider time dependent excited states, it gets more difficult to find a definite connection between the optimized Euclidean path integral and its gravity dual, mainly because there is no criterion about how to choose nice time slices. Nevertheless, a natural generalization of our previous argument is that for each of the time slices, we can associate a Euclidean path integral with a position dependent UV cutoff.

E. Lorentzian AdS/CFT

So far we have discussed an interpretation of AdS/CFT for the Euclidean AdS$_3$. As a next step we move on to the Lorentzian AdS$_3$, which is the main focus in the rest of this paper. In Lorentzian AdS/CFT, we expect that each codimension two surface corresponds to a quantum state

with the unit norm as argued in [18], called surface/state correspondence. Therefore, in AdS$_3$, the evolution of a closed curve on a time slice corresponds to that of quantum states and we expect that this is described by a continuous version of tensor network. Indeed, as shown in [31,32], a procedure called tensor network renormalization tells us that the Euclidean path integral can be (up to overall normalization) well approximated by the MERA network [4]. It is intriguing to note that this tensor network renormalization looks very analogous to our procedure of Euclidean path integral summarized in Fig. 1, though the former is formulated in the language of tensor networks.

Since the (minimum) time slice in the Euclidean AdS$_3$ is the same as that in the Lorentzian one, we expect that the time slice in Lorentzian AdS$_3$ corresponds to a tensor network for the CFT vacuum which can be approximated by the MERA. We can apply the same argument for time independent excited states in holographic CFTs (i.e. primary states and their descendants).

Consider an analytical continuation from the Euclidean AdS$_3$ to Lorentzian one. If we perform the Wick rotation $(\tau, \eta) \to (\tau, i\eta + i\pi/2)$, then the Euclidean AdS$_3$ metric (16) is mapped to the Lorentzian one with the hyperbolic slices (13), while the shift $(\tau, \eta) \to (\tau + i\pi/2, \eta + i\pi/2)$ maps (16) into the de Sitter slices (11). If we take an analytical continuation of the UV cutoff function (30) on the hyperbolic slice in Euclidean AdS$_3$, we find for the Lorentzian AdS$_3$

$$\text{hyperbolic slices}: \Gamma\left(\frac{k_{H_2} \cdot z}{\sin \eta} \right),$$
$$\text{de Sitter slices}: \Gamma\left(\frac{k_{dS_2} \cdot z}{\sinh \eta} \right). \qquad (39)$$

It has been pointed out that the MERA has a causal structure [13–16], which may suggest an identification of the MERA space with a de Sitter space. This occurs if we fix all the tensors of the MERA and change a quantum state in the UV as the propagation of the change is limited to a region whose boundary looks like a light cone. However, it is not clear how this is related to any causality in itself gravity dual interpretation. Indeed, if we consider an excitation in the bulk AdS, it is expected to correspond to a modification of a tensor in the middle of a MERA network following a similar idea in [19]. Under this modification of the tensor, the UV quantum state, which is obtained by contracting all tensors in the MERA, is modified at any point and there are no causal cones. At the same time, our Euclidean path-integral approach does not have any causal cone structure, as the excitation in the middle of the path integral can lead to the backreactions at any points under our optimization procedure. In this sense, our Euclidean path-integral description fits more nicely with the hyperbolic slices.

In order to have direct contact with explicit field theories, we work with a continuum version of tensor network with

UV cutoff, rather than explicit lattice models. Therefore we study a continuous description of tensor network, especially focusing on the cMERA [10]. Indeed in the next section we see that for the free scalar example, the length scale dependent wave function (22) is essentially the same as that in a cMERA description.

IV. CMERA

In this section we review the formulation of the cMERA for CFTs [10] with several elaborations e.g. constructions of the cMERA for a massless scalar field theory on a circle and details of the spacelike scaling operation, aiming at an interpretation of Lorentzian AdS/CFT.

A. Construction of the cMERA

The formulation of the cMERA was originally introduced in [10] for field theories on the noncompact spacetime R^{d+1}. We start from the IR state $|\Psi_{\text{IR}}\rangle$ which is completely disentangled so that its real space entanglement vanishes below the UV cutoff scale. To fix our convention we write the lattice constant as ϵ which is the inverse of the UV cutoff $\Lambda = 1/\epsilon$. As in the MERA [4], we add the entanglement at each length scale and perform the coarse graining until we finish this procedure at the UV cutoff scale.

We specify the length scale by u such that this corresponds to the coarse graining by the factor e^u. This parameter u takes the values from $u = -\infty$ (IR limit) to $u = 0$ (UV limit). A spacial region with the linear size y in the UV theory ($u = 0$) is regarded as that with the linear size ye^u at the scale u. Note that we keep the UV cutoff ϵ unchanged. Therefore the number of lattice sites gets decreased as e^{du} when we go from UV to IR. Therefore when the space manifold on which our field theory is defined is compact, the lattice points get trivialized in the IR limit. Therefore we can regard $|\Psi_{\text{IR}}\rangle$ as a disentangled state with no real space entanglement. For CFTs on noncompact spacetimes such as R^{d+1}, there is a subtlety to define $|\Psi_{\text{IR}}\rangle$ as the number of lattice sites is still infinite even in the IR limit. Therefore in this case $|\Psi_{\text{IR}}\rangle$ turns out to be equal to the CFT vacuum $|0\rangle$ (for the modes below the UV cutoff scale, i.e. $k \leq \Lambda = 1/\epsilon$). As analyzed in [10] if we introduce a massive deformation, this subtlety does not happen and $|\Psi_{\text{IR}}\rangle$ is given by the disentangled state.

The operation (so-called entangler) which adds entanglement is written as $K(u)$, which is an integral of an operator which is local below the UV cutoff scale ϵ. The coarse-graining operation is described by L, which is a spacelike (nonrelativistic) scale transformation as we see later in more detail. The state at scale u, denoted by $|\Psi(u)\rangle$ is expressed as follows:

$$|\Psi(u)\rangle = P \exp\left[-i\int_{-\infty}^{u} d\tilde{u}(K(\tilde{u}) + L)\right]|\Psi_{\text{IR}}\rangle. \quad (40)$$

As mentioned earlier, for CFTs on R^{d+1}, the IR state $|\Psi_{\text{IR}}\rangle$ is equal to the vacuum $|0\rangle$.

One immediately notices that the choice of $K(u)$ has huge ambiguities if we just fix the IR state and UV state. There are infinitely many ways to interpolate the two states. However, for a CFT vacuum state, we can choose a special one owing to the conformal symmetry. This canonical choice is such that $K(\tilde{u}) + L$ coincides with the dilatation operator or equally relativistic scale transformation denoted by L' for the modes below the UV cutoff scale. Explicitly, we have $L' = \int dx^d \sum_{i=1}^{d} T_{tx_i} x^i$, using the energy stress tensor $T_{\mu\nu}$. Above the UV cutoff scale $k > \Lambda = 1/\epsilon$, we set $K = 0$, while L is still present. For the details of this refer to the original paper [10] and further studies in [16]. In most parts of our arguments we do not write the higher modes explicitly. Thus in the cMERA construction we have that $|\Psi(u)\rangle$ is given by the CFT vacuum below the UV cutoff scale.

It is sometimes useful to introduce the "interaction picture" counterpart of the above cMERA formulation based on the state $|\Phi(u)\rangle$ [11], which is simply related to $|\Psi(u)\rangle$ via

$$|\Psi(u)\rangle = e^{-iuL}|\Phi(u)\rangle. \quad (41)$$

This state is expressed as follows:

$$|\Phi(u)\rangle = P \exp\left[-i\int_{-\infty}^{u} d\tilde{u}\,\hat{K}(\tilde{u})\right]|\Phi_{\text{IR}}\rangle, \quad (42)$$

where we defined $\hat{K}(u) = e^{iuL}K(u)e^{-iuL}$. In this description, the effective momentum cutoff is u dependent as Λe^u, while the size of the space manifold does not change. In this description of the compactification radius does not depend on u.

B. Free massless scalar field theory

Consider an example of free massless scalar field theory on R^{d+1}. We rewrite the original formulation of [10] in terms of creation and annihilation operators as in [11]. The Hamiltonian of this theory is defined by

$$H = \frac{1}{2}\int dk^d[\pi(k)\pi(-k) + |k|^2\phi(k)\phi(-k)]. \quad (43)$$

We can define the creation and annihilation operator of the scalar field, a_k and $a_k^\dagger$, as follows,

$$\phi(k) = \frac{a_k + a_{-k}^\dagger}{\sqrt{2|k|}},$$

$$\pi(k) = \sqrt{2|k|}\left(\frac{a_k - a_{-k}^\dagger}{2i}\right), \quad (44)$$

so that they satisfy $[a_k, a_{k'}^\dagger] = \delta^d(k - k')$.

In the description by $|\Psi(u)\rangle$, the action of the operation $K + L = L'$ for the modes below the UV cutoff scale (i.e. $k \leq \Lambda = 1/\epsilon$), which is equal to the relativistic scale transformation, is defined by

$$L' = -\frac{1}{2}\int dx^d \left[\pi(x)x\partial_x\phi(x) + x\partial_x\phi(x)\pi(x) \right.$$
$$\left. + \frac{d-1}{2}\phi(x)\pi(x) + \frac{d-1}{2}\pi(x)\phi(x) \right], \qquad (45)$$

and leads to the action on the annihilation operator (similarly on the creation operator)

$$e^{-iuL'}a_k e^{iuL'} = e^{-\frac{d}{2}u}a_{ke^{-u}}. \qquad (46)$$

Note that in the two-dimensional case, which we are interested in our paper, L' coincides with the dilatation charge $\int dx T_{tx}x$ as expected.

The nonrelativistic and relativistic scale transformation are defined as follows [10],

$$L = -\frac{1}{2}\int dx^d \left[\pi(x)x\partial_x\phi(x) + x\partial_x\phi(x)\pi(x) \right.$$
$$\left. + \frac{d}{2}\phi(x)\pi(x) + \frac{d}{2}\pi(x)\phi(x) \right], \qquad (47)$$

and its action is given by

$$e^{-iuL}a_k e^{iuL} = e^{-\frac{d}{2}u}(\cosh(u/2)a_{ke^{-u}} + \sinh(u/2)a^\dagger_{-ke^{-u}}). \qquad (48)$$

In the description by $|\Phi(u)\rangle$, the IR state $|\Phi_{\text{IR}}\rangle$ should be a state with no real space entanglement. It can be constructed as the ground state of the highly massive Hamiltonian $H_\Lambda = \frac{1}{2}\int dx[\pi(x)^2 + \Lambda^2\phi(x)^2]$ because in the IR limit the Hamiltonian becomes infinitely many copies of harmonic oscillators corresponding to each lattice point. This state is invariant under the transformation by L and is constructed explicitly as follows. The ground state condition is written as $a_x|\Phi_{\text{IR}}\rangle = 0$, where $a_x = \sqrt{\Lambda}\phi(x) + \frac{i}{\sqrt{\Lambda}}\pi(x)$ is the annihilation operator in real space. By taking Fourier transformation, we can express it as

$$|\Phi_{\text{IR}}\rangle = \prod_{k<\Lambda}|\Omega^k_\Lambda\rangle, \qquad (49)$$

where $|\Omega^k_\Lambda\rangle$ is defined by the condition

$$(\alpha_k a_k + \beta_k a^\dagger_{-k})|\Omega^k_\Lambda\rangle = 0, \qquad (50)$$

where

$$\alpha_k = \frac{1}{2}\left(\sqrt{\frac{\Lambda}{|k|}} + \sqrt{\frac{|k|}{\Lambda}} \right),$$
$$\beta_k = \frac{1}{2}\left(\sqrt{\frac{\Lambda}{|k|}} - \sqrt{\frac{|k|}{\Lambda}} \right). \qquad (51)$$

Assuming that the state is "Gaussian," the entangler $\hat{K}$ (42) takes the following form,

$$\hat{K}(u) = \frac{i}{4}\int dk^d \Gamma(ke^{-u}/\Lambda)(a^\dagger_k a^\dagger_{-k} - a_k a_{-k}); \qquad (52)$$

$\Gamma(x)$ is the cutoff function such that $\Gamma(x) = 1$ when $x \leq 1$ and $\Gamma(x) = 0$ for $x > 1$. This operation $\hat{K}$ induces the correct Bogoliubov transformation which maps the IR disentangled state $|\Phi(-\infty)\rangle = |\Phi_{\text{IR}}\rangle$ into the CFT vacuum $|\Phi(0)\rangle = |0\rangle$. More explicitly we find

$$|\Phi(u)\rangle \propto \left[\prod_{k<\Lambda e^u} \exp\left(\tanh\frac{u}{2}a^\dagger_k a^\dagger_{-k} \right)|0_k\rangle \right] \cdot \left[\prod_{k>\Lambda e^u} |\Omega^k_\Lambda\rangle \right]. \qquad (53)$$

On the other hand, $|\Psi(u)\rangle$ is explicitly given by

$$|\Psi(u)\rangle = \left[\prod_{k<\Lambda}|0_k\rangle \right] \cdot \left[\prod_{k>\Lambda}|\Omega^k_\Lambda\rangle \right]. \qquad (54)$$

Remember that even though the right-hand side looks u independent, the definition of momentum k is u dependent such that the actual unit length scale between lattice sites grows like e^{-u}. Therefore, the UV cutoff Λ corresponds to the actual momentum scale Λe^u. In addition, $|\Omega^k_\Lambda\rangle$ represents a trivial state with no real space entanglement. Therefore we can identify that the quantum state defined by the wave function Ψ_z (22) essentially coincides with the cMERA state $|\Psi(u)\rangle$ (54).[3] Combined with the argument in the previous section based on the Euclidean path integral, this observation strongly suggests that the hyperbolic time slice in the Lorentzian AdS spacetime corresponds to the cMERA.

---

[3]To see this explicitly, after the shift of momentum $k \to ke^u$ with the standard identification $z_0 = \epsilon \cdot e^{-u}$, the quantity inside the exponential in (22) becomes $\int_{-\Lambda/\lambda}^{\Lambda/\lambda} dk|k|(1 - e^{-2/\lambda+2|k|\epsilon})\varphi(k)\varphi(-k)$. For $|k|\epsilon \ll 1$ we have the vacuum state, while for $|k| > \Lambda$ we have the trivial wave function corresponding to the Neumann boundary state [33,34]. As we discuss as the example (i) in Appendix A, we can improve the high momentum behavior of the cutoff function and realize the state $|\Omega_\Lambda\rangle$ for $|k| \gg \Lambda$. The one other choice (ii) in Appendix A, or equally (23) and (24), leads to the Dirichlet boundary state $|B_D\rangle$ for $|k| \gg \Lambda$, which is similar to a version of the cMERA considered in [35]: $|\Psi(u)\rangle = [\prod_{k<\Lambda}|0_k\rangle] \cdot [\prod_{k>\Lambda}|B_D\rangle]$.

C. Compactification and spacelike scale transformation

For the purpose of this paper, it is very useful to compactify the space coordinates. For simplicity, we focus on two-dimensional CFTs on $R \times S^1$, where the space coordinate is compactified on a circle S^1. We take the radius of the circle in the original UV theory to be R_0. In the $|\Psi(u)\rangle$ picture, the radius depends on u as $R(u) = R_0 e^u$, while in the $|\Phi(u)\rangle$ picture, the radius is independent from u as $R(u) = R_0$.

Now we turn to the spacelike scale transformation L. In general QFTs, we argue that the L action is simply given by a specific quantum quench where the metric in the space direction changes,

$$
\begin{aligned}
H &= H_0 + \int dx^d \sum_{i,j=1}^{d} \delta g_{ij} T^{ij} \\
&= H_0 - \int dx^d \sum_{i,j=1}^{d} \delta g^{ij} T_{ij},
\end{aligned}
\tag{55}
$$

where we take

$$
\delta g_{ij} = 2\eta \delta_{ij}.
\tag{56}
$$

This shift of Hamiltonian changes the radius R into $R(1+\eta)$.

For example, consider a free scalar field CFT $\phi(t,x)$ in two dimensions. The action looks like

$$
S = \int dt dx \left[\frac{1}{2} (\partial_t \phi)^2 - \frac{1}{2R^2} (\partial_x \phi)^2 \right],
\tag{57}
$$

and the Hamiltonian is found to be ($\pi = \dot{\phi}$)

$$
H = \int dx \left[\frac{1}{2} \pi^2 + \frac{1}{2R^2} (\partial_x \phi)^2 \right].
\tag{58}
$$

We compactify the space coordinate x such that $x \sim x + 2\pi$. Then the radius is given by R. The mode expansion of the scalar field is given by

$$
\begin{aligned}
\phi(x,t) &= \sqrt{R} \sum_{n \in Z} \frac{1}{\sqrt{|n|}} [e^{-inx - i\frac{|n|}{R}t} a_n + e^{-inx + i\frac{|n|}{R}t} a_{-n}^\dagger], \\
\pi(x,t) &= \frac{i}{\sqrt{R}} \sum_{n \in Z} \sqrt{|n|} [-e^{-inx - i\frac{|n|}{R}t} a_n + e^{-inx + i\frac{|n|}{R}t} a_{-n}^\dagger],
\end{aligned}
\tag{59}
$$

where the canonical commutation relation is given by

$$
[a_n, a_m^\dagger] = \delta_{n,m}.
\tag{60}
$$

Consider a quench process where we suddenly change the radius R into R' at $t = 0$. If we define the creation and annihilation operator in the new theory by b_n and $b_n^\dagger$, by matching ϕ and π at $t = 0$ we find

$$
\begin{aligned}
\sqrt{R}(a_n + a_{-n}^\dagger) &= \sqrt{R'}(b_n + b_{-n}^\dagger), \\
\frac{1}{\sqrt{R}}(a_n - a_{-n}^\dagger) &= \frac{1}{\sqrt{R'}}(b_n - b_{-n}^\dagger).
\end{aligned}
\tag{61}
$$

Now, the transformation e^{-iuL} changes the radius from R to Re^u. Thus if we set $R' = Re^u$ we find the transformation

$$
a_n = \cosh\frac{u}{2} \cdot b_n + \sinh\frac{u}{2} \cdot b_{-n}^\dagger,
\tag{62}
$$

which agrees with (48).

This leads to the following transformation rule:

$$
e^{-iuL} a_n e^{iuL} = \cosh(u/2) a_n + \sinh(u/2) a_{-n}^\dagger.
\tag{63}
$$

Indeed this reproduces the noncompact limit result (48) by setting $k = n/R$.

As we have explained before, below the u dependent UV cutoff

$$
n \le R_0 e^u / \epsilon,
\tag{64}
$$

we simply have $|\Psi(u)\rangle = |0\rangle$ in the $|\Psi(u)\rangle$ picture[4] [or equally see (54)]. This is obvious from the L' action (below the UV cutoff scale),

$$
e^{-iuL'} a_n e^{iuL'} = a_n.
\tag{66}
$$

In this free scalar model, we can confirm[5]

$$
[L, l_n] = 0, \quad \text{and} \quad [K, l_n] = [K + L, l_n] = 0,
\tag{67}
$$

where $l_n \equiv L_n - \tilde{L}_{-n}$. L_n and $\tilde{L}_n$ are the Virasoro generators in the left and right-moving sector and they are explicitly given by

$$
L_n = \frac{1}{2} \sum_{m \in Z} \alpha_m \alpha_{n-m}, \qquad \tilde{L}_n = \frac{1}{2} \sum_{m \in Z} \tilde{\alpha}_m \tilde{\alpha}_{n-m},
\tag{68}
$$

---

[4]In the $|\Phi(u)\rangle$ description, we find the constraint $(\cosh(u/2) a_n - \sinh(u/2) a_{-n}^\dagger)|\Phi(u)\rangle = 0$. Thus we can identify (here again we omit the higher momentum modes $n > R_0 e^u / \epsilon$)

$$
|\Phi(u)\rangle = \exp\left(\tanh\frac{u}{2} \sum_{n < R_0 e^u / \epsilon} a_n^\dagger a_{-n}^\dagger \right)|0\rangle.
\tag{65}
$$

[5]Note that the latter two identities in (67) only hold below the UV cutoff scale.

where we defined α_n and $\tilde{\alpha}_n$ such that when $n > 0$, $i\alpha_n = \sqrt{n}a_n$ and $i\tilde{\alpha}_n = \sqrt{n}a_{-n}$ and that when $n < 0$, $-i\alpha_n = \sqrt{-n}a_{-n}^{\dagger}$ and $-i\tilde{\alpha}_{-n} = \sqrt{n}a_n^{\dagger}$.

We expect that these properties are true in the general cMERA for two-dimensional CFTs. In the IR limit ($u \to \infty$), $|\Psi(u)\rangle$ approaches an L invariant state: $L|\Psi(-\infty)\rangle = 0$. Therefore we expect from (67) that it satisfies the following identity:

$$l_n|\Psi(-\infty)\rangle = 0. \quad (69)$$

Thus $|\Psi(-\infty)\rangle$ is given by a boundary state.[6] Since we do not expect any excitation of the primary state, it is natural to identify it with an Ishibashi state [33] for the vacuum sector [12,35].

Even if we ignore the connection to the cMERA, our argument here shows the following intriguing fact: the evolution from the CFT vacuum to the Ishibashi state $|\Phi_{\text{IR}}\rangle$ is realized as a quantum quench induced by the radius change.

V. CONTINUOUS TENSOR NETWORKS AND AdS$_3$/CFT$_2$

In the paper [18], it has been conjectured that there is a holographic map between any codimension two convex surface Σ in a gravitational spacetime and a quantum state in a dual Hilbert space, called surface/state correspondence. This generalizes the standard holographic principle as the gravitational spacetime does not necessarily need the presence of a boundary. If we apply this duality to the AdS$_3$/CFT$_2$, we find that each convex closed curve Σ corresponds to a quantum state $|\Psi(\Sigma)\rangle$ in the dual CFT Hilbert space. By considering a foliation by closed curves, we obtain a tensor network for each codimension one slice in AdS$_3$. We gave a general formulation of the continuous tensor in Appendix B. Clearly, a particularly simple and nice example of the codimension one slice is the time slice $t = $ const which we study in detail below.

This surface/state correspondence was originally motivated by assuming a possible description of gravitational spacetimes by ideal tensor networks. Later in [12], this tensor network was argued to be described by the cMERA mainly from the viewpoint $|\Phi(u)\rangle$ description. Here we study this issue of AdS$_3$/CFT$_2$ in the $|\Psi(u)\rangle$ picture.

Our argument in this section goes as follows. We start with the surface/state correspondence for AdS$_3$/CFT$_2$. Using the Killing symmetry and its holographic counterpart in CFT$_2$ we construct a continuous tensor network. Next we show that this tensor network actually coincides with that of the cMERA with the canonical choice of K (below the cutoff scale).

---

[6]In the definition of (50), it corresponds to the Neumann boundary condition.

A. Constructing a continuous tensor network from AdS$_3$/CFT$_2$

Now we construct a continuous tensor network which describes the global AdS$_3$ spacetime (3) via the surface/state correspondence. We focus on the closed curve defined by a constant value of ρ on the time slice $t = 0$. We write the corresponding state parametrized by the value of ρ as $|\Psi(\rho)\rangle$. The dual CFT in AdS$_3$/CFT$_2$ lives on the boundary of AdS$_3$ parametrized by the boundary coordinate (t, ϕ) and the radius R of space coordinate ϕ is $R = 1$. If we express the UV cutoff of CFT as that of the AdS space given by $\rho = \rho_{\infty}(\to \infty)$, the quantum state $|\Psi(\rho)\rangle$ is defined in the Hilbert space of dual CFT on R $\times$ S^1 with the radius of circle S^1 given by

$$R(\rho) = \frac{\sinh \rho}{\sinh \rho_{\infty}}. \quad (70)$$

Note that this Hilbert space is always regularized by a lattice spacing ϵ which does not depend on ρ. The UV state $|\Psi(\rho_{\infty})\rangle$ should coincide with the CFT vacuum $|0\rangle_{R=1}$, where we make the radius explicit as a subscript. The state at general ρ can be written in the following form:

$$|\Psi(\rho)\rangle = P \exp\left[-i \int_0^{\rho} d\tilde{\rho} M(\tilde{\rho})\right] |\Psi(0)\rangle. \quad (71)$$

We determine the ρ evolution operator $M(\rho)$ by employing the $SL(2, R)$ symmetry we discussed just before. First remember that

$$l_n = L_n - \tilde{L}_{-n}$$
$$= -\int_0^{2\pi} d\phi e^{in\phi} T_{--}(\phi) + \int_0^{2\pi} d\phi e^{in\phi} T_{++}(\phi), \quad (72)$$

where $T_{\mu\nu}$ is the energy stress tensor of the two-dimensional CFT.

In order to find $M(\rho)$ we evaluate ∂_{ρ} for the infinitesimally short interval $\phi_0 - \delta/2 \le \phi \le \phi_0 + \delta/2$. This leads to

$$M(\rho) = \int_0^{2\pi} d\phi_0 M(\rho, \phi_0),$$
$$M(\rho, \phi_0) = \frac{1}{\delta} \int_{-\delta/2}^{\delta/2} d\phi \sin(\phi)(-T_{--}(\phi_0 + \phi)$$
$$+ T_{++}(\phi_0 + \phi)),$$
$$= \frac{1}{\delta} \int_{-\delta/2}^{\delta/2} d\phi \sin(\phi) T_{t\phi}(\phi_0 + \phi)$$
$$\simeq \frac{1}{\delta} \int_{-\delta/2}^{\delta/2} d\phi \phi T_{t\phi}(\phi_0 + \phi) \simeq D(\phi_0), \quad (73)$$

where D is the dilatation operator. This agrees with the cMERA for the Poincare AdS space near the AdS boundary as L' is the relativistic scale transformation as we noted

before. If we perform integration of ϕ_0 to find $M(\Sigma_\rho)$ we simply find

$$M(\rho) = 0, \qquad (74)$$

in the $\delta \to 0$ limit. This can also be found from the total derivative structure

$$M(\rho, \phi_0) \simeq \frac{\delta^2}{12} \partial_\phi T_{t\phi}|_{\phi=\phi_0}, \qquad (75)$$

in the $\delta \to 0$ limit. This trivial evolution (74) agrees with the free scalar construction on a cylinder (66). Since this property is also true in the cMERA for any CFT, we find that our cTN which is obtained from AdS_3/CFT_2 agrees with that of the cMERA with the canonical choice of entangler K via the identification of radius

$$R_0 e^u = \frac{\sinh\rho}{\sinh\rho_\infty} = R(\rho). \qquad (76)$$

Here we need to understand that this correspondence is confirmed below the UV cutoff scale ($k < \Lambda$) as we do not know how to probe quantum states from AdS_3 above the cutoff scale ($k > \Lambda$) at present. The quantum state $|\Psi(\rho)\rangle$ of the network for the CFT vacuum is simply given by

$$|\Psi(\rho)\rangle = |0\rangle_{R(\rho)}, \qquad (77)$$

where $|0\rangle_R$ denotes the vacuum for the CFT on a cylinder with radius R.

In the above argument, we consider a deformation of the AdS boundary into a smaller circle with the rotational symmetry. More generally, we can consider any deformation without any rotational symmetry by locally acting ∂_ρ and ∂_ϕ in principle such as the action $\int_0^{2\pi} d\phi_0 [A(\phi_0)\partial_\rho + B(\phi_0)\partial_\phi]$. This leads to a state $|\Psi(\Sigma)\rangle$ for any closed curve Σ, which realizes the idea of surface/state correspondence.

B. Other slices

So far we focused on the cTN on the hyperbolic plane H_2 defined as the time slice $t = 0$. On the other hand, the space built from the MERA network is often associated with a de Sitter space [13–16]. Therefore it is useful to consider what kind of cTN we can obtain from de Sitter slices.

We can find a one parameter family of de Sitter slices [see (11)] defined by

$$\cosh\rho \sin t = \cosh\eta_0, \qquad (78)$$

where η_0 is a positive constant. This is a two-dimensional de Sitter space (dS_2) with the metric

$$ds^2 = L^2 \sinh^2\eta_0 (-d\tau^2 + \cosh^2\tau d\phi^2), \qquad (79)$$

embedded in AdS_3 and it approaches the $t = 0$ slice at the AdS boundary $\rho \to \infty$. We can confirm that the actions of $l_{\pm 1}$ and l_0 preserve the dS_2 (78) directly.[7] By generalizing (8) for nonzero t we find

$$-\frac{i}{2}(e^{i\phi}l_{-1} - e^{-i\phi}l_1) = i(\cos t\partial_\rho - \sin t\tanh\rho\partial_t) = i\partial_\tau. \qquad (80)$$

Thus as in the previous subsection, we can identify the τ evolution in (79) as the same operation (73). This shows that the cTN on the dS_2 can also be identified with the cMERA network. In this way, as far as we consider the CFT vacuum, the hyperbolic slice and de Sitter slice have the same symmetric properties and seem to be identified with the cMERA network. However, once we consider excited states in a holographic CFT, they lead to different cTN descriptions of an identical state as we see in Sec. VII.

We mention that in the de Sitter space, there is a nonzero minimum radius $\sinh\eta_0 > 0$. This hole in the center may lead to a problem if we regard the de Sitter space as a cMERA network. One possibility is that this might be related to the fact that the sub-AdS locality is not manifest in the cMERA. Another possibility is that this actually suggests that the interpretation of the cMERA in terms of a de Sitter space is not correct. We leave more investigation of this issue for future research. Note that in this paper our main framework is based on the identification of the cMERA as a hyperbolic slice in AdS space.

VI. AN ARGUMENT FOR SUB-ADS SCALE LOCALITY

So far, in our analysis of continuous tensor networks, we studied general two-dimensional CFTs and did not employ any special condition for holographic CFTs. Therefore, this is not enough to explain the sub-AdS scale locality [15,36]. Indeed, in our cMERA formulation, the momentum cutoff appears as follows:

$$n \lesssim \frac{R_0 e^u}{\epsilon} = \frac{\sinh\rho}{\epsilon\sinh\rho_\infty} \sim \sinh\rho, \qquad (81)$$

where we employed the cutoff (64) and the standard identification of the UV cutoff in AdS/CFT $\epsilon \sim e^{-\rho_\infty}$. Therefore when ρ is $O(1)$, we cannot distinguish the different points in the AdS_3 spacetime, thought the distance between such points is order $O(c)$ (c is the central charge of the two-dimensional CFT). This means a locality only at the AdS radius L scale.

However, a standard knowledge of AdS/CFT tells us that in holographic CFTs we can get a finer resolution of spacetime up to the Planck scale. Holographic CFTs are

---

[7]We are very grateful to Juan Maldacena for pointing out this.

characterized by the large central charge c and a large spectrum gap [24]. Here we turn to a simple tractable model which captures these properties: a symmetric product CFT with a large central charge c on a cylinder with the radius $R_0 = 1$, though this is not exactly a holographic CFT dual to a standard classical gravity, strictly speaking. Such a CFT can be expressed as M^m/S_m which is a symmetric product of m identical CFTs, each of which is denoted by M. We have $c = mc_M$, where c_M is the central charge of M. This theory is defined as an orbifold of M^m by the symmetric group S_m. Its twisted sectors include a so-called long string sector. If we write a primary field of the CFT M as $\phi(t, x)$, the long string sector is defined by a boundary condition like $\phi_a(t, x + 2\pi) = \phi_{a+1}(t, x)$, where $a = 1, 2, …, m$ distinguishes m copies of the CFT M.

In this model, the long string sector, which dominates the microstate degeneracy, can be effectively[8] described by a single CFT M on a cylinder with the extended radius mR_0 [25]. Thus this gives a very fine-grained momentum quantization $P = \frac{n}{m} (n \in Z)$ instead of $P = n$. After Fourier transformation, this leads to a network with a much finer structure by the factor $1/m = O(1/c)$. The resolution of this network is estimated as $L\epsilon \sinh\rho_\infty \cdot (1/c) \sim L/c$, which is indeed the Planck length scale. In other words, the actual lattice constant is estimated as ϵ/m instead of $\epsilon = \Lambda^{-1}$. This fact can also be explained schematically by folding a MERA network description for the long string sector as in Fig. 2.

The above is our heuristic argument for a sub-AdS locality in AdS$_3$/CFT$_2$. Note that in order to explain a similar locality in a higher dimensional AdS/CFT, we encounter a fractional power of central charge and this suggests that the characterization of holographic CFTs in higher dimensions is much more complicated.

VII. BULK LOCALLY EXCITED STATES AND THE CMERA

Now we turn to a description of excited states in terms of continuous tensor networks. Especially we focus on a class of excited states which correspond to simple excitations in the bulk AdS space, i.e. local excitations in the bulk. In the global AdS$_3$ we excite one point at a specific time. Using the symmetry of AdS$_3$ space, we can focus on an excitation at $\rho = t = 0$, constructed by acting a bulk scalar field φ_α on the bulk vacuum, i.e. $\varphi_\alpha|0\rangle_{\text{AdS}}$. The label α expresses the primary field in the two-dimensional CFT and the bulk scalar field is also labeled by α as φ_α. We denote the corresponding primary state in the CFT $|\alpha\rangle$ and we take its chiral and antichiral conformal dimension to be $h_\alpha = \bar{h}_\alpha$.

In [12] (see also [37] for a similar but different formulation), the CFT dual of such a excitation was

---

[8]This is clear from the boundary condition $\phi_a(t, x + 2m\pi) = \phi_a(t, x)$.

identified with the "global Ishibashi state" with the $\frac{\pi}{2}$ time translation denoted by

$$|\Psi_\alpha\rangle = e^{-\tilde{\epsilon}H}e^{-i\frac{\pi}{2}H}|J_\alpha\rangle, \qquad (82)$$

where $\tilde{\epsilon}$ is the UV regularization which makes the excited energy finite and $|J_\alpha\rangle$ is the Ishibashi state for the global conformal symmetry and satisfies

$$l_{\pm 1}|J_\alpha\rangle = l_0|J_\alpha\rangle = 0. \qquad (83)$$

On the other hand, the state $|\Psi_\alpha\rangle$ satisfies (in the limit $\tilde{\epsilon} \to 0$)

$$(L_{\pm 1} + \tilde{L}_{\mp 1})|\Psi_\alpha\rangle = 0,$$
$$(L_0 - \tilde{L}_0)|\Psi_\alpha\rangle = 0. \qquad (84)$$

More explicitly, $|J_\alpha\rangle$ is written as

$$|J_\alpha\rangle = \sqrt{\mathcal{N}} \sum_{k=0}^{\infty} e^{-\tilde{\epsilon}k}|k, \alpha\rangle, \qquad (85)$$

where

$$|k, \alpha\rangle = \frac{1}{N_k}(L_{-1})^k(\tilde{L}_{-1})^k|\alpha\rangle,$$
$$N_k \equiv \frac{\Gamma(k+1)\Gamma(2h_\alpha + k)}{\Gamma(2h_\alpha)}. \qquad (86)$$

This CFT dual of the bulk locally excited state is precisely identical to that obtained by acting the known CFT dual of the bulk local field (HKLL map) [38] on the vacuum state as shown in [12,39,40].

A. Continuous tensor network for bulk locally excited states

We construct continuous tensor networks which reproduce such locally excited states in the global AdS$_3$. In order to realize the UV state $|\Psi(u)\rangle$ other than the CFT vacuum state, we obviously need to modify the tensor operator $M(\rho)$ in (71). For example, in the cMERA for a free scalar field such a modification is solved for quantum quench excitations in [11]. In terms of the discretized tensor networks for lattice quantum systems, such modification is realized by changing tensors as in [19,41]. Especially if we excite a point in the bulk by a local field, we can obtain the tensor network by replacing a tensor located at the point where the local field is inserted as depicted in Fig. 3.

Below we construct a cTN for the locally excited state following this prescription. If we insert the bulk local field at $\rho = 0$, we can still use the same network with $M(\rho, \phi)$ given by (73) for $\rho > 0$. Since we have $M(\rho) = 0$ as we showed before, we can simply identify the state $|\Psi(\rho)\rangle$ with
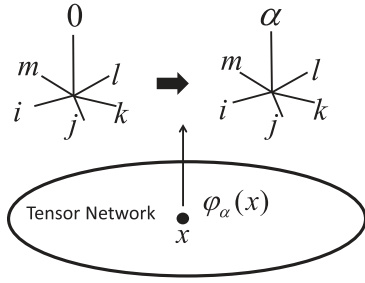
FIG. 3.   A modification of the tensor network dual to a bulk local excitation.

$$|\Psi(\rho)\rangle = |\Psi_\alpha\rangle_{R(\rho)}, \qquad (87)$$

so that it reproduces (82) in the UV limit $\rho = \rho_\infty$. Note that when $|\alpha\rangle$ is the CFT vacuum $|0\rangle$, this is trivially reduced to the network (77) for the vacuum which we discussed before.

Since we focused on the hyperbolic slice H_2 defined by $t = 0$ in the above, one may wonder how it looks if we choose other slices such as de Sitter slices. In the gravity dual, if we excite a point in the bulk, the excitation expands within a light cone as depicted in Fig. 4. Therefore we expect that the tensors which correspond to the inside light-cone region will be modified from those for the vacuum state. Since we do not have a systematic way to identify this deformation currently, we cannot closely follow cTN for general slices including de Sitter slices. In other words the hyperbolic slice has an advantage as we can only modify a single tensor (or equally the IR state) to describe the locally excited state.

Now we explore the consequence of the network flow (87) a bit more. Remember that the state $|\Psi_\alpha\rangle$ satisfies the condition (84). We notice that this is the global part of the standard property $(L_n - (-1)^n \tilde{L}_{-n})|C\rangle = 0$ of cross cap states $|C\rangle$ as noted in [39]. Moreover, if we consider the IR limit $\rho \to 0$, the allowed momentum modes are limited such that only $n = 1$ modes are meaningful as the radius $R(\rho)$ shrinks. Therefore, we can identify the IR state $\lim_{\rho \to 0} |\Psi_\alpha\rangle_{R(\rho)}$ as the cross cap states in holographic
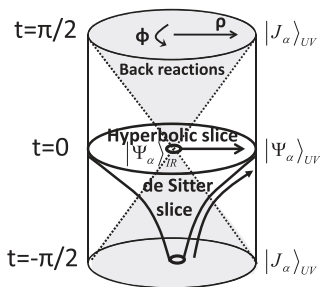

FIG. 4.   The tensor network evolutions which correspond to a locally excited state in global AdS$_3$.
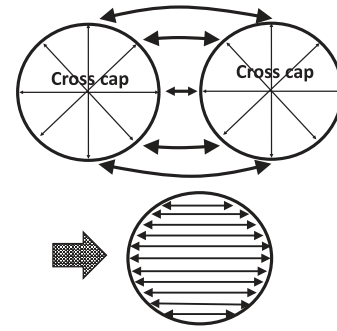

FIG. 5.   Gluing two cross cap states leads to an identity operation.

CFTs under a large c approximation. Notice that the cross cap state is a highly entangled state, while the boundary states are disentangled states [35]. Indeed, the latter is obtained from a time translation by $\pi/2$ of the latter state and the time evolution by $\pi/2$ leads to entanglement propagations to anywhere as is familiar in quantum quenches [42].

In the free field CFTs, we can impose complete conditions for cross cap states by relating a point and its antipodal point in terms of fundamental free fields [33,34], which leads to a maximally entangled tensor if we view a state as a tensor. If we paste two cross cap states more than half of each, we get the identity operation as explained in Fig. 5. This is the same property which the perfect tensor [19] (see also [43]) satisfies.

In the case of holographic CFTs, we only know the cross cap condition for the Virasoro generators and explicit computations look much more difficult. However, if we remember that the state is obtained from time evolution of a boundary state, the entanglement scrambling phenomenon found in [44] suggests that our cross cap states in holographic CFTs are no longer such simple entangled states as in free field CFTs but are more scrambled states, similar to the random tensors in [20].

VIII. CONCLUSION AND DISCUSSION

In this paper we studied connections between tensor networks and AdS/CFT from two different viewpoints. In the first part, we considered a Euclidean path-integral description of ground state wave functions in two-dimensional CFTs in the presence of the UV cutoff. We optimized the path-integral computation by introducing a position dependent UV cutoff without changing the final wave function. We found that this is regarded as a path-integral on a hyperbolic space and we argued that this space corresponds to a time slice of AdS. This conjecture is supported from the global symmetry of AdS$_3$ and also from the fact that such a field theory is expected to appear as a dual CFT on a hyperbolic space. By shifting its boundary, we defined a wave function as a function of effective length scale. This scale dependent wave function turns out to be

essentially the same as the evolution of quantum states in the cMERA at least below the cutoff scale. This observation leads to the interpretation of the hyperbolic time slice in (Euclidean) AdS spaces as a tensor network. It is an intriguing future problem to perform an explicit analysis of our discretized path integral in specific lattice models.

In the latter part, we took a different approach. We started with a Lorentzian AdS$_3$ and studied a systematic construction of continuous tensor network description dual to AdS$_3$/CFT$_2$ assuming the surface/state correspondence [18]. We obtained the resulting network for the canonical time slice, which is a hyperbolic space H_2, from gravitational considerations and found that it essentially coincides with the (compactification of) the original cMERA network [10]. However, notice that our analysis from AdS$_3$ geometry only concerns the modes below the cutoff scale.

Interestingly, through an analysis of the locally excited bulk state, we observed that our network is very analogous to the perfect tensor network [19] and random tensor network [20]. This is because the IR state is given by $\pi/2$ time translation of the boundary state, where nontrivial quantum entanglement is generated. We also gave a heuristic argument of the sub-AdS scale bulk locality in the cMERA, based on symmetric product CFTs. All these suggest that the cMERA, which has full conformal invariance manifestly, can be regarded as a continuous refinement of tensor networks such as the perfect and random tensor network and thus is expected to describe a canonical time slice of AdS space at least below the cutoff scale.

The Wick rotation from the Euclidean AdS space to the Lorentzian AdS space is obvious for the canonical time slice $t = 0$. The above arguments, i.e. the correspondence between a Euclidean path integral on H_2 with a UV cutoff and the cMERA network, are based on this fact. However, if we choose other hyperbolic slices [$\eta \neq 0$ in (16)] in Euclidean AdS space, they can be Wick rotated into hyperbolic (13) or de Sitter (11) slices. This implies that the cMERA network can also be interpreted as a de Sitter slice. Indeed, our analysis based on the Killing vectors in AdS space and its CFT dual supports this possibility. This might make some connection to a seeming independent idea based on kinematic spaces [14]. However at the same time we noticed that the existence of the minimal radius, which looks like an IR cutoff, in de Sitter geometry is confusing from the viewpoint of the cMERA. This issue certainly deserves future investigations.

In this paper we mainly consider two-dimensional CFTs for simplicity. However, notice that most results can be generalized into the higher dimensional AdS/CFT in a straightforward way.

Finally it is a very interesting future problem to find an explicit relation between the spacetime metric and the property of the continuous tensor network. An important challenge is to work out how we obtain the timelike component of the metric.

APPENDIX A: OTHER CHOICES OF UV CUTOFF FUNCTION

Here we consider more general (position dependent) UV cutoff functions in the Euclidean path integrals of a free scalar and compute resulting scale dependent wave functions, which generalizes our result in (22). Here we set $\lambda = 1$. Since we do not want to change the low momentum ($|k|z < 1$) behavior we only modify the higher energy part, keeping the scaling symmetry as follows:

$$\Gamma(|k|z) \rightarrow f(|k|z) \equiv \Gamma(|k|z) + (1 - \Gamma(|k|z)) \cdot g(|k|z). \tag{A1}$$

The wave function at the length scale z_0 is expressed as

$$\Psi_{z_0} = \exp\left(-4\pi \int_{-\infty}^{\infty} dk c(k) \phi(k) \phi(-k)\right), \tag{A2}$$

where

$$c(k) = |k|^2 \int_{z_0}^{\infty} dz f(|k|z) \cdot e^{-2|k|(z-z_0)}. \tag{A3}$$

In the expression of creation/annihilation operators, this wave function is equivalent to the quantum state

$$|\Psi_{z_0}\rangle \propto \exp\left(-\int_0^\infty dk\left(\frac{8\pi c(k)-|k|}{8\pi c(k)+|k|}\right)a_k^\dagger a_{-k}^\dagger\right)|0\rangle. \quad (A4)$$

When $g(|k|z) = 0$, we have $c_0(k) = \frac{|k|}{2}(1-e^{2|k|z_0-2})$, which precisely corresponds to (22). Below we consider two other choices. First consider the case (i) $g(|k|z) = \frac{\beta_1}{|k|z}$, where β_1 is a constant. In this case we obtain

$$c(k) = c_0(k) + \alpha \cdot \beta_1 \cdot |k| \cdot e^{2|k|z_0} \quad (\text{if } |k|z_0 < 1),$$
$$= \beta_1 |k| \int_0^\infty \frac{dy}{y+z_0} e^{-2|k|y} \quad (\text{if } |k|z_0 > 1), \quad (A5)$$

where α is a positive constant given by the integral $\int_1^\infty \frac{dy}{y} e^{-2y}$. When $|k|z_0 \gg 1$ we can approximate

$$c(k) \simeq \frac{\beta_1}{2z_0}. \quad (A6)$$

This behavior coincides with the IR state $|\Omega_\Lambda\rangle$ used in the original cMERA [10] [see (54)], after the rescaling $ke^u \to k$ or equally $z_0 \to \Lambda$. Thus in the connection to the cMERA, this choice gives a refinement of (22).

On the other hand, if we consider the second choice (ii) $g(|k|z) = \beta_2 e^{|k|z-1}$ (β_2 is an arbitrary constant), we find

$$c(k) = c_0(k) + \beta_2 |k| \cdot e^{2|k|z_0-2} \quad (\text{if } |k|z_0 < 1),$$
$$= \beta_2 |k| \cdot e^{|k|z_0-1} \quad (\text{if } |k|z_0 > 1). \quad (A7)$$

In particular, we choose $\beta_2 = 1/2$. Since in this case we get $c(k) = \frac{|k|}{2}$ for $|k|z_0 < 1$, this precisely reproduces the correct vacuum wave function (21) in the limit $z_0 = 0$. Since $c(k)$ grows exponentially, for a high momentum $|k|z_0 \gg 1$ it approaches a boundary state (Ishibashi state) for the Dirichlet boundary condition. In the Euclidean path integral, this choice of UV cutoff can suppress high momentum modes as the scalar field action S becomes very large. In this sense, it is similar to the Wilsonian renormalization group flow. These observations are consistent with the recent paper [21].

APPENDIX B: SPACETIME CONTINUOUS TENSOR NETWORK

Here we summarize a formulation of the cTN, which generalizes the cMERA formulation so that we can apply it to non-AdS spacetimes. Surface/state correspondence [18] argues that any gravitational spacetime can have such a tensor network description. We start with a $d+2$-dimensional gravitational spacetime M_{d+2} described by Einstein gravity.

We choose a coordinate $x = (t, \vec{x}) \in M_{d+2}$ for simplicity, though our argument below should be independent from the choice of coordinate. At a point x, we associate an entangling Hermitian operator $M_i(x)$ ($i = 1, 2, ..., d+1$), which is local up to the UV cutoff scale dual to the Planck length. The index i describes the spacial direction of the entangling operation. The time evolution of $M_i(x)$ is simply given by a Hamiltonian $H(x)$ at each point which satisfies

$$\frac{dM_i(x)}{dt} = i[H(x), M_i(x)]. \quad (B1)$$

Now we take a time slice (codimension one spacelike surface) N_{d+1} and consider its one parameter foliation by codimension two surfaces Σ_u i.e. $N_{d+1} = \cup_u \Sigma_u$. The surface/state duality tells us that there is a corresponding state for each surface,

$$\Sigma_u \leftrightarrow |\Psi(\Sigma_u)\rangle. \quad (B2)$$

Here we assume that the homology Σ_u is trivial so that it is dual to a pure state.

We can write the u evolution as

$$|\Psi(\Sigma_{u_1})\rangle = P \cdot \exp\left(-i\int_{u_2}^{u_1} du M(\Sigma_u)\right)|\Psi(\Sigma_{u_2})\rangle. \quad (B3)$$

Our basic claim is that $K(\Sigma_u)$ is expressed in terms of the local entangler $M_i(x)$ as follows,

$$M(\Sigma_u) = \int_{x \in \Sigma_u} dx^d n_u^i(x) M_i(x), \quad (B4)$$

where n_u^i is the displacement vector of Σ_u when we change u at x.

From (B4) we obtain the important consistency condition of our spacetime tensor network,

$$\frac{dH(x)}{du} = i[n_u^i(x) M_i(x), H(x)]. \quad (B5)$$

Consider various choices of foliations of the time slice N_{d+1}. We take two of them, expressed as Σ_u and Σ_w such that $N_{d+1} = \cup_u \Sigma_u = \cup_w \Sigma_w$. Let us assume that $\Sigma_{u_1} = \Sigma_{w_1} \equiv \Sigma_1$ and $\Sigma_{u_2} = \Sigma_{w_2} \equiv \Sigma_2$.

Correspondingly we have two expressions

$$|\Psi(\Sigma_1)\rangle = P \cdot \exp\left(-i\int_{u_2}^{u_1} du M(\Sigma_u)\right)|\Psi(\Sigma_2)\rangle,$$
$$= P \cdot \exp\left(-i\int_{w_2}^{w_1} dw M(\Sigma_w)\right)|\Psi(\Sigma_2)\rangle. \quad (B6)$$

Since we expect the same thing is also true for excited states which are obtained by replacing some of the tensor inside $\Sigma_2(\in \Sigma_1)$ locally, we require

$$P \cdot \exp\left(-i\int_{u_2}^{u_1} du M(\Sigma_u)\right)$$
$$= P \cdot \exp\left(-i\int_{w_2}^{w_1} dw M(\Sigma_w)\right). \qquad (B7)$$

From this, we can conclude that $M(\Sigma)$ is a flat connection in the space of codimension two surfaces in M_{d+2}. Therefore we can write K as

$$M(\Sigma_u) = i\partial_u G(u) \cdot G(u), \qquad (B8)$$

for a certain unitary matrix valued function $G(u)$. Then the state dual to the surface is written in the form

$$|\Psi(\Sigma_u)\rangle = G(u)|\Psi^{(0)}\rangle, \qquad (B9)$$

where $|\Psi^{(0)}\rangle$ is a certain reference state. $G(u)$ for any codimension two surfaces in M_{d+2} defines the continuous tensor network.

[1] G. 't Hooft, Dimensional reduction in quantum gravity, arXiv:gr-qc/9310026; L. Susskind, The world as a hologram, J. Math. Phys. (N.Y.) **36**, 6377 (1995); D. Bigatti and L. Susskind, TASI lectures on the holographic principle, arXiv:hep-th/0002044.

[2] J. M. Maldacena, The large N limit of superconformal field theories and supergravity, Adv. Theor. Math. Phys. **2**, 231 (1998); The large N limit of superconformal field theories and supergravity, Int. J. Theor. Phys. **38**, 1113 (1999).

[3] B. Swingle, Entanglement renormalization and holography, Phys. Rev. D **86**, 065007 (2012); Constructing holographic spacetimes using entanglement renormalization, arXiv:1209.3304.

[4] G. Vidal, A Class of Quantum Many-Body states that can be Efficiently Simulated, Phys. Rev. Lett. **101**, 110501 (2008).

[5] G. Vidal, Entanglement Renormalization, Phys. Rev. Lett. **99**, 220405 (2007); Entanglement renormalization: an introduction, arXiv:0912.1651; G. Evenbly and G. Vidal, in *Strongly Correlated Systems. Numerical Methods*, edited by A. Avella and F. Mancini, Springer Series in Solid-State Sciences Vol. 176 (Springer, New York, 2013).

[6] S. Ryu and T. Takayanagi, Holographic Derivation of Entanglement Entropy from the anti–de Sitter Space/ Conformal Field Theory Correspondence, Phys. Rev. Lett. **96**, 181602 (2006); Aspects of holographic entanglement entropy, J. High Energy Phys. 08 (2006) 045; V. E. Hubeny, M. Rangamani, and T. Takayanagi, A covariant holographic entanglement entropy proposal, J. High Energy Phys. 07 (2007) 062.

[7] M. Van Raamsdonk, Lectures on gravity and entanglement, arXiv:1609.00026.

[8] M. Rangamani and T. Takayanagi, Holographic entanglement entropy, arXiv:1609.01287.

[9] M. Freedman and M. Headrick, Bit threads and holographic entanglement, arXiv:1604.00354.

[10] J. Haegeman, T. J. Osborne, H. Verschelde, and F. Verstraete, Entanglement Renormalization for Quantum Fields, Phys. Rev. Lett. **110**, 100402 (2013).

[11] M. Nozaki, S. Ryu, and T. Takayanagi, Holographic geometry of entanglement renormalization in quantum field theories, J. High Energy Phys. 10 (2012) 193.

[12] M. Miyaji, T. Numasawa, N. Shiba, T. Takayanagi, and K. Watanabe, Continuous Multiscale Entanglement Renormalization Ansatz as Holographic Surface-State Correspondence, Phys. Rev. Lett. **115**, 171602 (2015).

[13] C. Beny, Causal structure of the entanglement renormalization ansatz, New J. Phys. **15**, 023020 (2013).

[14] B. Czech, L. Lamprou, S. McCandlish, and J. Sully, Integral geometry and holography, J. High Energy Phys. 10 (2015) 175; Tensor networks from kinematic space, J. High Energy Phys.07 (2016) 100.

[15] N. Bao, C. Cao, S. M. Carroll, A. Chatwin-Davies, N. Hunter-Jones, J. Pollack, and G. N. Remmen, Consistency conditions for an AdS multiscale entanglement renormalization ansatz correspondence, Phys. Rev. D **91**, 125036 (2015).

[16] A talk given by G. Vidal (based on joint work with Qi Hu), in It from Qubit Summer School, Perimeter Institute.

[17] B. Czech, L. Lamprou, S. McCandlish, B. Mosk, and J. Sully, A stereoscopic look into the bulk, J. High Energy Phys. 07 (2016) 129.

[18] M. Miyaji and T. Takayanagi, Surface/state correspondence as a generalized holography, Prog. Theor. Exp. Phys. (**2015**) 073B03.

[19] F. Pastawski, B. Yoshida, D. Harlow, and J. Preskill, Holographic quantum error-correcting codes: Toy models for the bulk/boundary correspondence, J. High Energy Phys. 06 (2015) 149.

[20] P. Hayden, S. Nezami, X. L. Qi, N. Thomas, M. Walter, and Z. Yang, Holographic duality from random tensor networks, J. High Energy Phys. 11 (2016) 009.

[21] J. R. Fliss, R. G. Leigh, and O. Parrikar, Unitary networks from the exact renormalization of wave functionals, arXiv:1609.03493.

[22] J. M. Maldacena and A. Strominger, AdS(3) black holes and a stringy exclusion principle, J. High Energy Phys. 12 (1998) 005.

[23] J. Polchinski, *String Theory. Vol. 1: An Introduction to the Bosonic String* (Cambridge University Press, Cambridge, 1998).

[24] T. Hartman, C. A. Keller, and B. Stoica, Universal spectrum of two-dimensional conformal field theory in the large c limit, J. High Energy Phys. 09 (2014) 118.

[25] J. M. Maldacena and L. Susskind, D-branes and fat black holes, Nucl. Phys. **B475**, 679 (1996).

[26] A. Karch and L. Randall, Locally localized gravity, J. High Energy Phys. 05 (2001) 008.

[27] O. Aharony, D. Marolf, and M. Rangamani, Conformal field theories in anti–de Sitter space, J. High Energy Phys. 02 (2011) 041.

[28] W. Li and T. Takayanagi, Holography and Entanglement in Flat Spacetime, Phys. Rev. Lett. **106**, 141301 (2011).

[29] N. Shiba and T. Takayanagi, Volume law for the entanglement entropy in nonlocal QFTs, J. High Energy Phys. 02 (2014) 033.

[30] J. M. Maldacena, Eternal black holes in anti–de Sitter, J. High Energy Phys. 04 (2003) 021.

[31] G. Evenbly and G. Vidal, Tensor Network Renormalization, Phys. Rev. Lett. **115**, 180405 (2015).

[32] G. Evenbly and G. Vidal, Tensor Network Renormalization Yields the Multiscale Entanglement Renormalization Ansatz, Phys. Rev. Lett. **115**, 200401 (2015).

[33] N. Ishibashi, The boundary and cross cap states in conformal field theories, Mod. Phys. Lett. A **04**, 251 (1989).

[34] J. L. Cardy, Boundary conditions, fusion rules, and the Verlinde formula, Nucl. Phys. **B324**, 581 (1989).

[35] M. Miyaji, S. Ryu, T. Takayanagi, and X. Wen, Boundary states as holographic duals of trivial spacetimes, J. High Energy Phys. 05 (2015) 152.

[36] T. Hartman and J. Maldacena, Time evolution of entanglement entropy from black hole interiors, J. High Energy Phys. 05 (2013) 014.

[37] H. Verlinde, Poking holes in AdS/CFT: bulk fields from boundary states, arXiv:1505.05069; A. Lewkowycz, G. J. Turiaci, and H. Verlinde, A CFT perspective on gravitational dressing and bulk locality, J. High Energy Phys. 01 (2017) 004.

[38] A. Hamilton, D. N. Kabat, G. Lifschytz, and D. A. Lowe, Local bulk operators in AdS/CFT: A boundary view of horizons and locality, Phys. Rev. D **73**, 086003 (2006); Holographic representation of local bulk operators, Phys. Rev. D**74**, 066009 (2006).

[39] Y. Nakayama and H. Ooguri, Bulk locality and boundary creating operators, J. High Energy Phys. 10 (2015) 114; Bulk local states and cross caps in holographic CFT, J. High Energy Phys.10 (2016) 085.

[40] K. Goto, M. Miyaji, and T. Takayanagi, Causal evolutions of bulk local excitations from CFT, J. High Energy Phys. 09 (2016) 130.

[41] X. L. Qi, Exact holographic mapping and emergent spacetime geometry, arXiv:1309.6282.

[42] P. Calabrese and J. L. Cardy, Evolution of entanglement entropy in one-dimensional systems, J. Stat. Mech. (2005) P04010.

[43] A. Bhattacharyya, Z. S. Gao, L. Y. Hung, and S. N. Liu, Exploring the tensor networks/AdS correspondence, J. High Energy Phys. 08 (2016) 086.

[44] C. T. Asplund, A. Bernamonti, F. Galli, and T. Hartman, Entanglement scrambling in two-dimensional conformal field theory, J. High Energy Phys. 09 (2015) 110.